ISSN 0006-3509, Biophysics, 2022, Vol. 67, No. 2, pp. 300–319. © Pleiades Publishing, Inc., 2022.
Russian Text © The Author(s), 2022, published in Biofizika, 2022, Vol. 67, No. 2, pp. 386–408.

COMPLEX SYSTEMS BIOPHYSICS

Hybrid Model of the Collapse of the Commercial Crab *Paralithodes camtschaticus* (Decapoda, Lithodidae) Population of the Kodiak Archipelago

A. Yu. Perevaryukha[a,*]

[a] *St. Petersburg Federal Research Center, Russian Academy of Sciences, St. Petersburg, 199178 Russia*
**e-mail: temp_elf@mail.ru*

Received December 11, 2021; revised December 17, 2021; accepted December 19, 2021

Abstract—Degradation of commercial populations remains a frequent phenomenon even with the use of methods of stocktaking and control of production volume. In fish farming, the concept of "overfishing" is used with and the signs of this condition are well known. However, the processes leading to the degradation of reserves develope in various ways. According to the theory of nonlinear dynamical systems, several types of crisis development can be classified. Of particular interest are the phenomena of collapse, that is, variants of a rapid decline in numbers, which are unexpected for the organizations controlling the fishery. Immediately before the collapse, the state of the stock can be assessed as relatively stable and it may experience fluctuations. Contrary to expectations, there was no rapid recovery after a rapid reduction in cod, whitefish *Coregonus clupeaformis* of the Great Lakes, halibut and other valuable species. This paper considers a hybrid model for the collapse of red king crab *Paralithodes camtschaticu*s stocks of the Kodiak archipelago of Alaska with unusual distinctive oscillating dynamics. The computational scenario in a hybrid system with survival and growth equations considers the logic of decision-making in operation management. The scenario differs in that after the fall of catches, the crab population goes into the sporadic fluctuations that do not have a regular character and are not characteristic of the population. The collapse itself occurs after a long interval of fishing while the population is in an unstable mode. The analysis shows that a long species life cycle is not a decisive factor for eliminating the risk of a collapse scenario. The presence of reserve generations does not change the situation qualitatively, the efficiency of their reproduction in crab and cod off the coast of Labrador turned out to be unexpectedly low. The status of stocks of large predators that require seasonal moratoriums on fishing must be regularly checked.

Keywords: nonlinear dynamics of ecosystem degradation, scenario modeling, management of biological resources exploitation, population collapse scenarios, irregular fluctuations and cycles, red king crab *Paralithodes camtschaticu*s population crisis

DOI: 10.1134/S0006350922020166

The properties of oscillating phenomena in the dynamics of various biological processes were investigated in our previous studies using mathematical methods. It was possible to describe damping fluctuations for a series of decreasing peaks of outbreaks of insect pests in boreal forests [1]. Transient oscillatory regimes leading to a "bottleneck" population crisis after the active phase of aggressive invasion were considered [2]. The oscillating process, unsteady in amplitude, is illustrated by modern epidemic dynamics. In many countries, the incidence records of COVID-19 have taken the form of a series of "waves" rolling in at intervals of four and a half months. For example, this happens in the United States, according to statistics given (Fig. 1). The waves cause an important psychological problem when victory over the epidemic seems very close, but it is suddenly necessary to reintroduce restriction regimes.

The regime of "epidemic waves" with an interval of four to six months is common; however it is not the only possibility for the development of this scenario. Epidemic processes and mortality rates differed significantly in different regions. In some countries, residents are more susceptible to the disease than in others. As an example, in Belgium, with 80% vaccination of citizens aged 18+, mortality remains slightly higher than in Slovakia with a vaccination rate of 54%. These obvious differences are interesting when considering people from the same ethnic group who live permanently in different regions. Our hypothesis about the immunological cause of such noticeable differences due to the influence of the spread of seasonal coronaviruses in the past, proposed in the spring of 2020 [1], has been substantiated. Cross-reactive immune T-cells

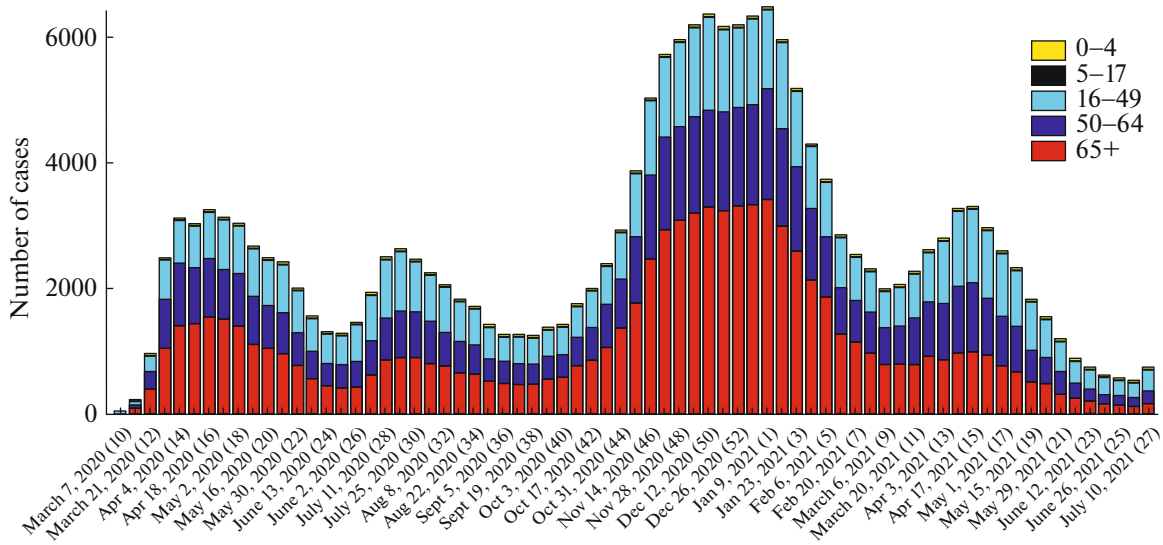

Fig. 1. The dynamics of waves of hospitalization of patients diagnosed with COVID-19 in all states of the United State per week from 03/7/2020 by age groups. (https://gis.cdc.gov/grasp/covidnet).

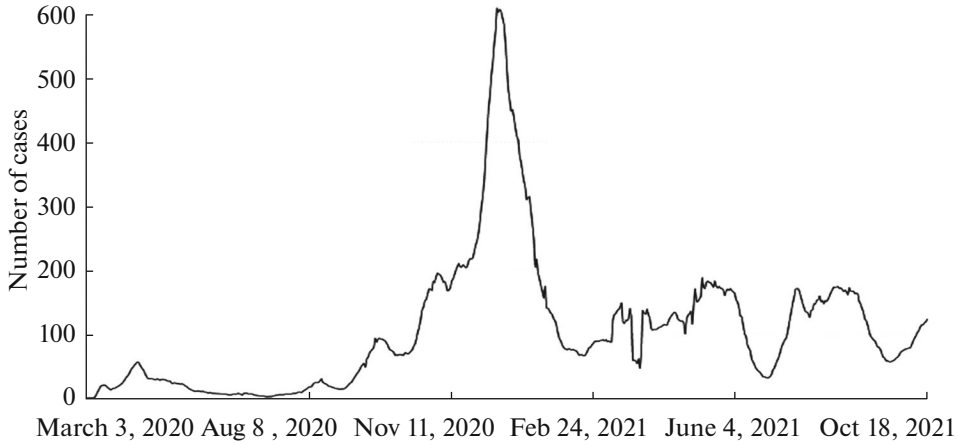

Fig. 2. The dynamics of COVID-19 infection cases in Denmark (monitored every case) per week with a pronounced peak in December 2020 (https://coronavirus.jhu.edu).

were also detected, and a universal immunodominant peptide was identified [3].

Many more studies will be focused on the analysis of the causes of the differences in the nature of local epidemics and their modeling. We have seen a brief outbreak of infections in Denmark, turning into sporadic dynamics without distinct periodic effects. There is an interesting aspect of the generality of nonlinear effects for biocybernetics. The epidemic scenario in Denmark shown on the graph in Fig. 2 is dynamically similar to the pattern of the development and rapid completion, in a month, of the breeding outbreak in psyllids of the genus Cardiaspina in Australia with the threshold launch scenario and with the probability of repetition of the Λ-shaped peak in pests with stochastic population behavior [4].

The global dynamics of the pandemic at the end of October 2021 demonstrates an intermediate trend of decreasing cases of infection (and the proportion of deaths) in the phase of attenuation of the third wave. A number of countries are breaking out of the trend of decreasing mortality in the autumn wave of 2021, where restrictions have been re-introduced and then canceled. In other regions, the beginning of the next phase of infection growth was observed; the dynamics was asynchronous. According to the graph shown in Fig. 3, it is already clear that the incidence at the peak of the fourth wave in Russia will significantly exceed the maximum of 2020.

The modifications of the SIR model of the epidemic proposed in the spring of 2020 could not predict the long oscillatory dynamics. The authors of [5] have

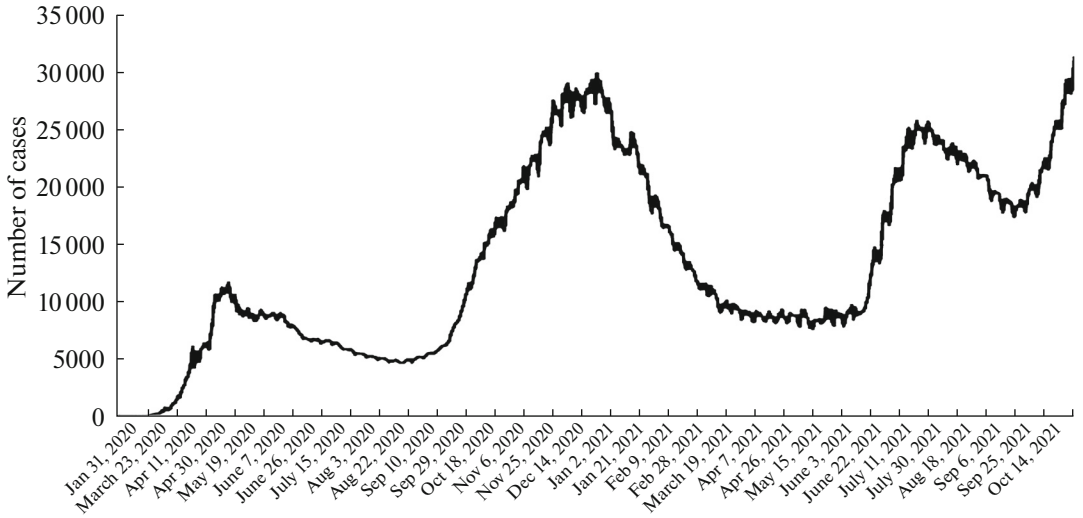

Fig. 3. The dynamics of COVID-19 epidemic waves in Russia according to official statistics of daily recorded cases of infection (https://coronavirus.jhu.edu).

proved that their system of equations did not have orbitally stable periodic solutions. Non-local SIR models with a solution in the form of traveling waves were being developed in 2021. Methods describing local flu outbreaks are not suitable for pandemic conditions. Historical analogies based on the "Spanish flu" and "swine flu" will not help model forecasts, since there were not four waves of previous flu pandemics. The pandemic of the "Russian flu" in 1889–1892 was most likely caused by the HCoV-OC43 coronavirus, which lost its pathogenicity in further evolution and transformed into four types; this was a way to reduce the pathogenicity of the virus to elude immunity.

The scenario of stepwise relaxation of oscillations without decreasing amplitude is unusual in biosystems, we can phenomenologically describe with the following equation:

$$\frac{dN}{dt} = rN(t)e^{-L[A(t)]}\left(\frac{K - N^2(t-\tau)}{(K + cN(t-\tau_1))^3}\right) \times (H - N(t-\tau)), \quad 0 < H < K. \qquad (1)$$

In equation (1), K is the value of the epidemic threshold for triggering an extreme increase in morbidity at $r > 1$; H is the pre-threshold state of accumulation of an active group of distributors. H acts in equation (1) with respect to the number of cases at some point earlier, lagging behind the average time interval of the latent stage of infection. According to the graph in Fig. 3, we estimate $H \approx 5000$. Including $e^{-L[A(t)]}$ as a damping functional sets the final attenuation of waves of any pandemic at $t \to \infty$. Theoretically, the effect is achieved with a threshold level of "collective immunity" $A(t)$ (according to various forecasts of experts this threshold is from 75% or even 92% in the population).

In the real scenario, instead of the attenuation phase of the third "wave", the fourth wave immediately began from the end of September, which indicates the effect of an additional disturbing factor of amplification of propagation. A similar dynamics of cyclical disruption by a sharp outbreak was observed in April 2021 in Brazil. Presumably, the cause was an "alarming" strain (Delta AY.4.2), however, it may be an unknown variant. The Delta variant originated in 2020. It was shown that the threat from Delta is associated with mutations not only of the *S* protein, but also with improvements in the structural *N* protein of the nucleocapsid, which increased the percentage of assembly of functional virions suitable for further infection inside the cell [6]. Only 1.5% of new virions are functional in HIV.

Mutations will continue to occur as random events in weakened host organisms; however, the selection factors of variants are not so stochastic and may change. For modeling, it is interesting that the accumulation of mutations in S1 was recorded at once. After multiple mutations, stability intervals followed. Adaptive evolution of the viral protein S1 subunit in 2020 was correlated with an increase in infectivity, via selection by affinity of its binding to the cellular receptor. A dangerous scenario is when the selection of mutations of the *S*-protein that overcome humoral immunity is provoked at low vaccination rates, that is, immunoglobulins will systematically begin to lose binding affinity to updated *S*-protein sites. The role of antibody-dependent amplification of infection in the development of the "cytokine storm" complication was analyzed [7, 8]. The ADE effect for COVID has so far been detected only in laboratory experiments with

animals [9]. The probabilistic ADE effect can lead to a cyclical local effect of an increase in morbidity in which the presence of antibodies developed earlier for some "drifting" antigens of old strains can become a negative factor in macrophage infection. The proposed solution to stop this process is revaccination of the population with vaccines of different technologies. In Chile, those who received the inactivated vaccine were given a third vaccination with a dose of mRNA vaccine.

A number of hypothetical methods of coronavirus inactivation have been discussed [10, 11]. In addition to the formation of long-term immunity due to CD8+ *T*-lymphocytes, the effect of the initial dose of infection on the dysregulation of the immune response [12, 13] and complications in COVID [14] remains unclear. In a dangerous scenario, the release of cytokines is initially slowed down due to the inhibition of interferon activity by auxiliary proteins of the virus; and then it sharply increases and launches an avalanche-like destructive positive feedback loop of the inflammatory reaction.

To describe the three different scenarios of epidemic dynamics shown on the graphs, it is necessary to use different special mathematical apparatus capable of generating the exact nonlinear effects we need. Their number is limited by fundamental theorems, which forces us to combine methods.

We will discuss another important situation of rapid changes in population processes, the phenomena of degradation with controlled intervention. The purpose of this work is to design a computational structure with an algorithmic representation of eventfulness in continuous time for scenario modeling of stock degradation options that occur as an unexpected collapse during controlled fishing. The dynamics of the development of marine fisheries crises, similarly to that of local epidemics, differs significantly from known examples; however, there are also some important aspects of similarity of situations in which we will compare nonlinear effects.

SCENARIOS OF COMMERCIAL DEGRADATION AND POPULATION COLLAPSE

Fishing regulated according to quotas of allowable catch often led to the degradation of biological resources, both local [15] and in a huge oceanic area [16]. The optimal exploitation of reserves is far from solved. Sometimes not even 30% of the estimated quotas allocated for fishing during an obvious crisis were used, as in the Caspian basin in 2006–2010 [17]. Both short-cycle species and large predators are subject to sharp degradation, but with significant differences in their recovery rates. Typing according to the similarity/difference in the stages of scenarios is interesting to us for analyzing the nonlinear dynamics of population crises. Cases with reliable estimates and catch data are important.

The most important aspect, which we mathematically drew attention to when comparing different cases is the degradation of biological resources that occurs either gradually with a small (<10%) annual loss, or in the form of a final collapse. The situation with the populations of sturgeon of the Caspian Sea is an example of degradation that has lasted for half a century; it was caused by excessive fishing and violation of the natural river flow of the Volga [18]. Since 2010 four species have been included as endangered species in the "Red Book". The official statistics shown in Fig. 4 [19] do not include illegal seizure. Now, in international documents, the UN calls on countries to fight *IUU*-fishing, that is, illegal, unregulated, and unreported fishing. It is necessary to know how much a subject has actually caught, even with the legal right to catch; moreover, for forecasting it is necessary to represent both the gender and size-age distribution of th individuals of the catch.

The reason for such a long depletion of stocks during predatory fishing is the complex intrapopulation structure of these fish with seasonal races [20] and the evolutionary adaptation of sturgeon to reproduction in limited channel spawning grounds [21, 22]. Subpopulation groups of fish entering the Volga or Ural rivers earlier or later than the main spawning group had chances to avoid fishing in the river; however, their efficiency of reproduction is lower than at the optimal flood level and temperature [23]. By analyzing the data on the migration of juveniles using moving average methods, we previously found the presence of two maxima for the indicator of spawning efficiency of the starry sturgeon *Acipenser stellatus* in the Volga. For the diamond sturgeon *Acipenser gueldenstaedtii*, a single domed maximum with an asymptote at a level that was half of the maximum was shown, and the shape of the curve of the dependence of the stock and replenishment of the beluga *Huso huso* did not have an extremum [24, 25]; however, our data interval was incomplete, since the stocks of beluga were depleted at the beginning of the 20th century.

A similar situation with a long 35 year degradation (according to [26, 27]) was observed for the zander *Stizostedion lucioperca* in the Sea of Azov. In the situation with sturgeon, there were opportunities to stop fishing long before the point of degradation. Artificial release of juveniles did not meet expectations for commercial return. The sharp collapse of stocks shown in Fig. 4 is fundamentally and obviously different from the prolonged monotonous depletion of valuable stocks. Population collapse is interpreted as a decrease in the number of adults by 90% in 3 years, and lasting for at least 10 years [28]. Many works have been devoted to cases of commercial collapse of hydrobionts, its causes and detectable signs for various objects of fishing, for example, for the mollusk *Chlamys islandica* [29]. A sche-

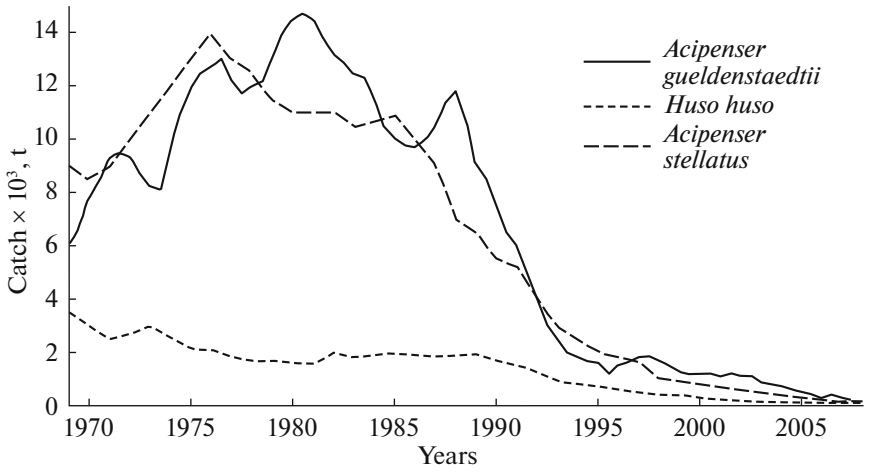

Fig. 4. The dynamics of degradation of three populations of Caspian Sea sturgeon (diamond sturgeon, starry sturgeon, and beluga) according to the volume of official catches [19].

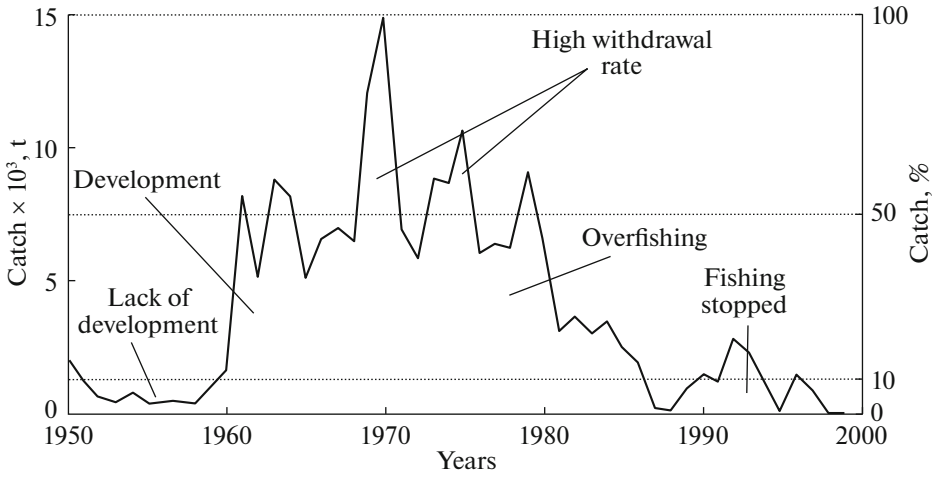

Fig. 5. The dynamics of catch for the general scenario of the stock collapse scheme (according to [30]).

matic diagram of the development of the collapse of stocks according to a catch schedule with an increase in the level of withdrawal, according toreview [30], is shown in Fig. 5. Immediately before the collapse, the catches had passed the peaks, but were still quite high. Consequently, such a hypothetical population could withstand a high level of withdrawal rate for a long time ($q > 0.6$), and this would be considered the norm. This is confirmed by the cases with Atlantic cod [31] and with the Volga starry sturgeon, where in some low-water years the withdrawal from the spawning part of the population reached up to $q \approx 0.8$. Hopes for a recovery reserve due to generations that have not yet entered the commercial age are eventually leveled by the long maturation of juveniles of these species, which will also face a suboptimal gender distribution due to different maturation times in males and females; this will represent generations with significantly different numbers at the time of the first spawning.

It was believed that short-cycle commercial species, such as the Peruvian anchovy *Engraulis ringens*, could be subject to a sharp but short reduction in stocks. The catches of the most fished fish in the world fell rapidly several times and recovered, but eventually decreased from a record 13 million tons in 1971 to 1.1 million tons by 2015, including due to the frequent occurrence of the warm El Nino current. Depletion of commercial stocks of Atlantic cod *Gadus morhua* off the coast of Canada was a crushing collapse in economic consequences due to the forced cessation of fishing since 1992 [32]. In addition, back in 1990, the forecasts here were favorable.

The provincial governments of Canada strictly regulate marine fishing; however, in the seasons immediately before the collapse, the quotas allocated were not

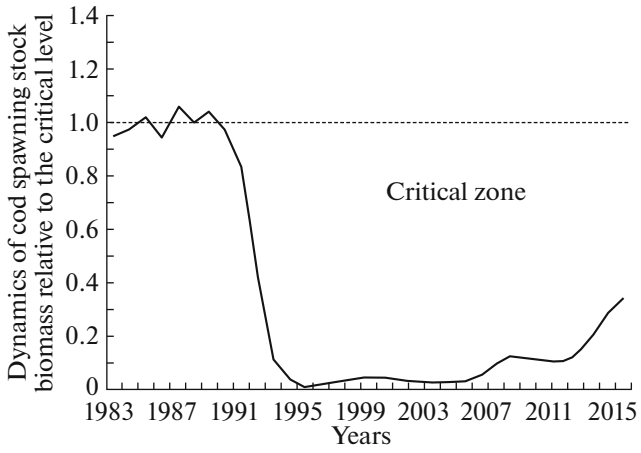

Fig. 6. The dynamics of the biomass of the cod spawning stock in the province of Newfoundland and Labrador relative to the critical LPR level (in million tons, according to estimates in [35]). Since 2015, there has been a steady increase in the spawning stock of the population and by 2030 we can expect to reach a critical level of the stock.

fully used, which indicates a systematic reassessment of the state of reserves. Many authors have discussed the degradation of this massive dominant predator in the waters of the provinces of Newfoundland and Labrador. The errors in the regulation of fishing, the unreliability of the assessment of the replenishment of generations due to the inaccuracy of accounting methods, the selectivity of the removal of large fish, and the accompanying natural factors of currents off the coast of North America were considered [33]. The selectivity of the removal of large and prolific individuals leads to a situation in which "stunted" and rapidly maturing genetic forms will prevail in the population; however, they are characterized by increased post-spawning mortality (an example known to fishermen is the Baltic smelt *Osmerus eperlanus* and its short-cycle lake form snetok).

Experts have not reached a consensus on the causes of the collapse for the cod case, although many versions and hypotheses have been put forward, includingjustifications of their miscalculations. A significant factor unaccounted for by fishing forecasts was the increased cannibalism of cod with an abundance of their own young. Initially, the regulatory authorities set a moratorium on cod fishing for 1.5 years. According to the most pessimistic expert forecasts, recovery after the collapse should have taken 9 years [34]; however, the fishery was not restored even after 20 years. It is the absence of the expected beginning of stock recovery according to model forecasts that is the main problem in the crisis scenario for large and long-lived species. The population was supposed to be restored quickly due to the hypothetically numerous reserve generations of cod still unused by the fishery; however, their numbers were unexpectedly not enough.

A graph of the dynamics of cod catches with a long-term stabilization interval between the peak of record catches and the collapse of the fishery in 1992 is available on Wikipedia. Here we show another, more interesting graph of the calculated dynamics of the biomass of the spawning stock of cod (Fig. 6). Modern estimates from [35] clearly confirm the threshold effect, which was previously difficult to explain for a multi-age stock.

After the degradation of the dominant predator population, changes occurred in the community of bottom hydrobionts. Fishing off the coast of Labrador has shifted to benthic invertebrates, which have increased biomass without the pressure from their main predator. The shrimps have become much larger. A similar situation was observed for the fauna in the Caspian Sea, where the fishing of large gobies began, they occupied a niche after the depletion of the stock of sturgeon, their predators and the main consumers of benthos. The size and age structure of mollusk populations that were previously consumed by sturgeon has changed. By 2000 large individuals began to predominate [36]. However, high productivity is provided by young organisms. Historically, the stocks of sturgeon fish were supported by a benthic feed base with low biomass, but with high productivity. The diet for juvenile sturgeon and cod has actually decreased.

From the point of view of nonlinear dynamics, a semi-stable equilibrium state was observed before the collapse of the cod, below which reproduction is reduced by a step function. Similar threshold transitions are already known in models for insect dynamics [37]. The situation with the forecast of cod stocks has been calculated many times; according to modern estimates, the fishing population will be restored by 2030 [38]. Analyzing several situations in different regions, we drew attention to the collapse development variants that are particularly interesting for mathematical biology.

THE SITUATION OF THE COLLAPSE OF THE COMMERCIAL CRAB POPULATION

Several situations of fishing collapse that differ in dynamics have happened; these collapse events attracted only local attention. Therefore, we analyzed a lesser known example of the dynamics of degradation of economically valuable stocks of a "non-fish" fishing object, which is interesting from the point of view of modeling.

Many populations have a natural oscillatory mode [39, 40]. At the same time, the duration of their oscillation period may not correlate with the length of the life cycle of the species itself [41]. As an example, in the case of cyclical outbreaks of the eastern spruce budworm *Choristoneura fumiferana* or quarter-century

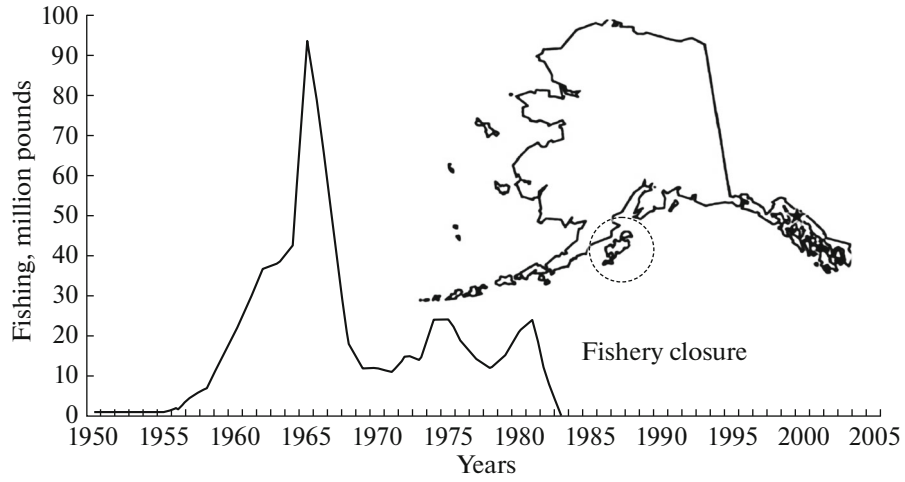

Fig. 7. The dynamics of *Paralithodes camtschaticus* crab fishing off the coast of the Aleutian Peninsula of Alaska and the islands of the Kodiak archipelago with collapse (according to [43]).

periods of fluctuations of the Far Eastern sardine *Sardinops melanostictus* [42] the cycles are not violated by the current global climate warming trend. The cycle can be an alternative stable mode of existence of the biosystem, along with equilibrium in a different range of the number of its components (in a different area of attraction of the attractor). The management problem is that the experts who determine the level of fishing withdrawal (seasonal quotas) are not ready for changes in natural trends. If experts have clearly observed a positive trend on the rising "wave" of the population cycle, they tend to extrapolate this trend in forecasts for the next seasons.

Figure 7 shows a schedule of fishing stocks of the Kamchatka crab *Paralithodes camtschaticus* (also known as "red king crab") with a final collapse by 1985 in the region of the Aleutian Peninsula of Alaska, in the Shelikhov Strait and the waters of the neighboring islands of the Kodiak Archipelago [43].

The crab population, which is numerous in the Pacific Ocean, has degraded over 35 years of fishing during quota-regulated and selective-sized fishing and has not recovered, despite all efforts. The peak of the crab catch was reached in 1966. As a result, the process from the peak of the catch to the point of collapse and the moratorium on fishing took almost 20 years (1966–1985). In this scenario, much more time passed before the collapse than in the case of cod in the waters of Labrador. Before the collapse, crab catches had been steadily growing to a local maximum for 5 years, the population was considered safe and there were no visible reasons for statisticians to adjust the withdrawal. The graph, which shows the dynamics of the catch mass (M, million pounds) of the Kodiak crab population, shows two sharp drops associated with a decrease in the stock S, when the quota was not mastered by fishing. The first 3.8-fold drop in catches occurred in 1968. A similar peak in catches with a sharp intermediate drop was also observed for Canadian cod. Between the crises, 17 years of crab fishing passed with 50% fluctuations in the catches. Recovery of crab stocks turned out to be more difficult than that of cod, and there is no data on the appearance of positive dynamics in this fishing area. The death of crabs in previously lost nets prevents recovery. The duration of the life cycle of the Kamchatka crab and cod of the Northwest Atlantic and their role as the dominant predator in the community (enhanced by cannibalism) are comparable.

Fishing is regulated for gourmet bottom invertebrates even more strictly than for mass commercial fish species, such as cod and anchovy, where the margin of error can be thousands of tons. However, it is possible to successfully plan future catches with a stable share of commercial return from the initial volumes of roe, and when the relationship between spawning stock and replenishment is successfully approximated by a fractional linear relationship. For sturgeon fish, the flood parameters calculated by the correlation method are used for correction. The management of the exploitation of biological resources becomes more complicated when the reproduction efficiency of a given population obeys an asymptotic dependence due to competition, which has extremes.

The case of crab collapse is mathematically more complicated. After the reduction of the number due to overfishing in 1965–1967, a sharp loss of equilibrium was obvious; however immediately an oscillatory mode of the stock size appeared between the first and final crisis of fishing. The scenario of local degradation of the Kamchatka crab population differs from the dynamics of the cod crisis in the large oscillating transition. For cod, pseudostabilization of the stock, which was in unstable equilibrium, was observed for a long time. If we compare the situations of known collapses with each other, then, from the point of view of

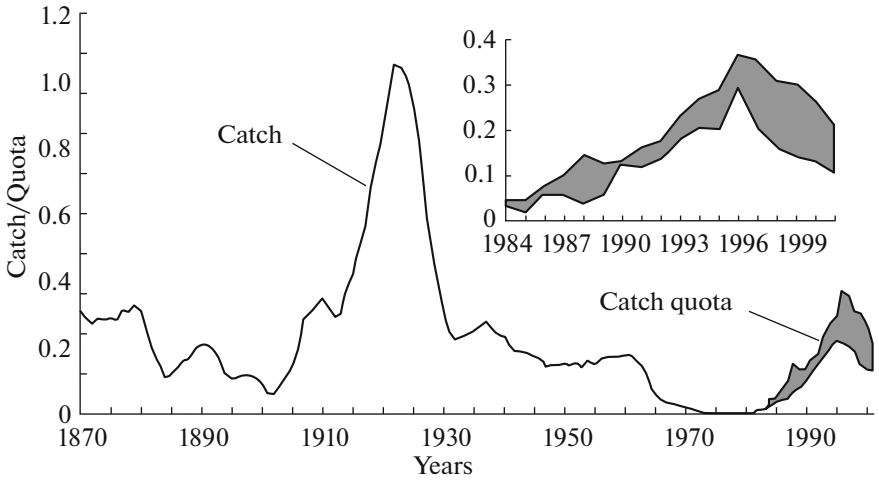

Fig. 8. The dynamics of whitefish catches in Lake Ontario (in million kg) with collapse in 1965 and population recovery by 1985, the catch quota is shown separately (according to [44]).

nonlinear dynamics, the visible metamorphoses of phase portraits have not only obvious similarities, but also some differences. In hydrobiont species that are very different taxonomically, the regulation of demographic processes can be reflected by a mathematically similar functional. It is the manifestation of threshold nonlinear effects and modes of sporadic fluctuations in the scenarios under consideration that make it unrealistic to establish a universal strategy for optimal fishing. It turned out to be difficult for statisticians to anticipate rapid collapse and understand its causes. Atlantic analogues are the cod *Gadus morhua* and the crab *Paralithodes camtschaticus*; these are long-lived large predators with a reserve of reproductive potential, as it was believed, they should not immediately collapse like anchovies.

Erroneous decisions in management theory can be both random and systematic. In order to confirm the hypothesis that the described scenario is not a consequence of a rare combination of circumstances at sea or an incident of displaying heterogeneously collected statistics, we will give another non-trivial example of a collapse that occurred after a pronounced peak catch and a subsequent 12-year fishing interval with an intermittent trend. A similar situation developed for the whitefish *Coregonus clupeaformis* in Lake Ontario with subsequent restoration (Fig. 8) [44]. This variant of the crisis requires a separate mathematical discussion, since there are accounting materials for the Great Lakes.

An additional factor of mortality unaccounted for in fishing forecasts in the case of whitefish in Lake Ontario was the invasion of a parasite, the sea lamprey *Petromyzon marinus*, into the Great Lakes. The lamprey was actively fought. After 20 years, the whitefish population began to recover, fishing was reopened; however, the allocated quota for catching again turned out to be excessive, and the situation with overfishing of whitefish was repeated, as predicted by the collapse schematic diagram in Fig. 5. Whitefish in some lakes has not recovered.

All three scenarios of degradation we have described are much more difficult for specialists making decisions about the level of exploitation than the persistent and long-lasting depletion of sturgeon stocks in the Caspian Sea.

We propose the construction of a discrete-continuous model for analyzing the dynamics of the transition from equilibrium to an oscillatory regime with a threshold collapse effect.

METHODOLOGY OF THE THEORY OF POPULATION REPLENISHMENT FORMATION

The justification of modeling with the inclusion of hybrid structures will be built within the methodology of the theory of replenishment formation. We will briefly outline the basic mathematical provisions of the concept and emphasize the non-obvious problems due to the use of this apparatus in evaluation of data about a dynamically changing object. The characteristics of reproduction efficiency in the collapse scenario should change with a large decrease in the stock relative to the historical optimum according to the inherent regulation functions, that is, first they should smoothly decrease, and then have a threshold effect that cannot be described in traditional models. The model should not require "external" parameter changes during calculations to describe the collapse.

The mathematical theory of the formation of replenishment of populations of hydrobionts was substantiated in [45, 46]. The main idea was formulated in the method of constructions based on observational data of the functional relationship between the existing parent stock and the replenishment received from spawning. It was assumed that if we estimate the form

of nonlinearity in the dependence, then it is possible to withdraw excess stock above the level of replenishment, the bisector of the coordinate angle [45]. In this case the optimal solution is obvious, namely, to transfer the stock S to a state S_{opt} when the position of the dependence curve over the bisector is largest, $D[f(S) - S] \to \max$. The approach does not work for all commercial species. The method of $f(S)$ curve analysis is more applicable to large species with large individual fertility, the effect of the stochasticity of environmental factors on which is less. Their stock status after the vulnerability interval is determined mainly by fishing and partly by post-spawning mortality. The taxonomic proximity of species does not guarantee similarity or the presence of visible dependencies; the level of competition for resources and survival factors of their young is more important. Cannibalism was considered to be one of the most important factors [45]. Intraspecies confrontation increases with a high stock density in spawning grounds, which was relevant for the species of the family Salmonidae studied in small rivers in Canada. The evolutionary adaptation of Caspian sturgeon was aimed at overcoming this factor, which used both remote migrations and spawning in the summer months to minimize competition. The overlap of migration routes leveled this adaptation.

If the reproduction conditions have changed dramatically, then the position of the extremes of the $f(S)$ dependence relative to the bisector transforms accordingly, and the maximum of the curve shifts to the left. Due to such factors of influence, more flexible methods are needed in calculations for the mathematical description of the variety of dependencies and the variability of the possible development of situations.

DYNAMIC PROPERTIES OF MODELS AND DATA ANALYSIS

A well-known reproduction function (replenishment of R from S) $R = f(S) = aS\exp(-bS)$ was proposed [45] with two parameters: reproductive parameter $a > 1$ and parameter $0 < b < 1$ that takes into account the effect of competition factors with increasing density. The nonmonotonicity of dependence is not only due to strong intraspecies competition between individuals for the best places during spawning in rivers, but also due to hypoxia [45]. With the redundancy of the roe in the stores, the dead roe becomes a source for the development of pathogenic microorganisms. The curve has one extreme maximum at $S = 1/b$ and a horizontal asymptote at $\lim_{S\to\infty} f(S) = 0$. Research in the search for methods to determine the dependence in the efficiency of reproduction continues [47, 48].

We are interested in the properties of reproduction models as dynamical systems with different attractors, and not in of the properties of approximating data sets to functional curves. The parameters are usually "unequal" in their influence on qualitative changes in phase portraits. In the iterative model $R_{n+1} = aR_ne^{-bRn}$ at $0 < a < e^2$, the trajectory generated by iteration from the R_0 starting point $\varphi^n(R_0 > 0)$ will have a single stable $\varphi(R^*) = R^*$ equilibrium position $R^* = (\ln a)/b > 0$. When increasing a to $a = e^2 + \varepsilon$, the R^* equilibrium will lose stability, $|f'(R^*)| > 1$. A cycle with a period of $p = 2$ will occur around an unstable stationary point. However, almost all points of R_0 are attracted to this cycle, except for R^* and all its point-prototypes $\varphi^{-n}(R^*)$. If a is further increased, the cycles of all powers of 2 will occur, $p = 2^i, i \to \infty$. These changes during bifurcations constitute a well-known "universal" chaotization scenario [49]. The finite increment of the parameter a leads to the period p becoming infinite. The cyclic points R_i^* that have lost stability are not attracted to the attractor. It is important to note that the sequences of bifurcations with $p = 2^{i+1}$ occur identically for all functions with a constant negative special ratio of the higher derivatives, the "Schwarzian". The characteristic of the function calculated with the second and third derivatives of $f(S)$, as well as the two Feigenbaum universality constants, do not have an ecological interpretation [50], they determine the type of behavior of iterations.

It is possible to discuss whether high reproductive potential or highly density-dependent mortality leads to randomization according to the model forecast. In fact, the mathematical theory of the formation of a global attractor in the form of a Cantor set based on the analysis of the renormalization of a group has no biological interpretation. In discrete models of biosystems it is better to avoided randomization according to M. Feigenbaum not because of the appearance of the chaos mode itself, but because of a number of effects of periodic windows. To do this, it is enough to violate the criteria of the doubling cascade with $p = \infty$; the most acceptable option is to specifically obtain alternative attractors for the trajectory $\varphi^n(R_0)$. A chaotic mode is possible without an attractor.

An alternative model of the nonlinear dependence "stock-replenishment" with a three-parameter functional iteration $R_{n+1} = aR_n/(1 + R_n/K)^b$ similarly experiences an infinite cascade of bifurcations of doubling the period; only randomization will occur with an increase in the parameter $b > 1$, which sets the intensity of the impact of compensatory mortality (increasing with increasing density). In a model without extremes of bifurcations, the birth of cycles does not occur, there is only equilibrium (possibly trivial) and any trajectory tends to it.

Note that the construction of the $f(S)$ curve based on observational data is a fundamentally hard to solve task. Regression methods were proposed [45]. How-

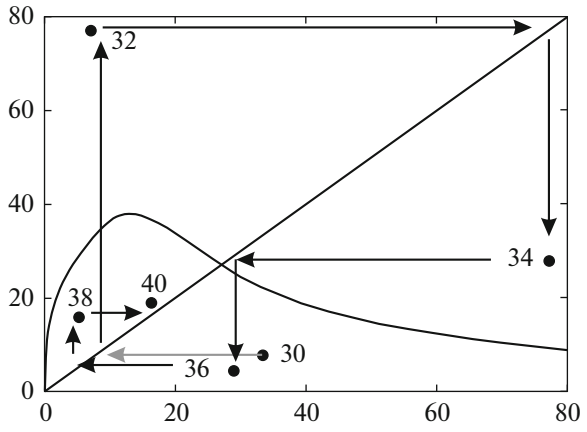

Fig. 9. The data on the dynamics of the pink salmon stock with atrajectory that we added and the "stock–replenishment" dependence constructed by the Ricker regression method [51].

ever, for dynamic systems, the approximation of elliptical point thickenings of any curve will not give any prognostic possibilities. In discrete dynamics, cyclic trajectories (sequences of repeating points) do not look like ellipsoids from continuous models. Imagine that a population is a natural dynamic system that develops according to some mathematical law, the evolution operator φ. The state in which the population occurs as a result of this dependence is limited to a subset in the phase plane (the behavior is dissipative). Eventually, the values of the stock quantity are compressed into a subdomain of the phase space, the neighborhood of a stable equilibrium state or a limit cycle of a finite period; however, the image points remain within a limited subset of $\Upsilon \pm \varepsilon$ on the phase plane $R \times S$.

The trajectories of discrete dynamical systems have attracting sets that can be topologically equivalent for various functional dependencies. The set of topological types of attractors is limited. Figure 9 shows an example graph on the $R \times S$ plane with data on the number of pink salmon with a 2-year life cycle in a river with a hypothetical dome-shaped replenishment curve constructed by the author [51]. We have added a trajectory in the form of a Lamerea diagram. Obviously, there is dependence between adjacent generations of pink salmon, otherwise the points would not lie under the arrows from the bisector; however, the complex dynamics cannot be explained by constructing such a curve. The iteration of the function with one maximum drawn by the author of [51] here simply has a stable stationary point, the intersection with the bisector (the angle of inclination of the tangent is slightly less than $\pi/4$). The stability criterion for point R^*, the calculated modulus of the derivative at this point, is less than one $|\varphi(R^*)| < 1$. With an increase in the angle of inclination of the tangent $>\pi/4$, a short cycle would occur; however, none of the points present in the figure fall into the area of the graph where the points of such a cycle could be located.

According to our assumption, the curve for the data in Fig. 9 should have both a maximum and a minimum, and the left branch should increase asymptotically at $f(S) < S$. The dynamics of pink salmon can often become aperiodic. A model based on $R_{n+1} = aR_n e^{-bRn}$ with $a > 40$ in a chaotic mode was proposed to describe changes in fluctuation trends in "even" and "odd" populations of the pink salmon *Oncorhynchus gorbuscha* of adjacent years [52].

It is impossible to restore the form of the "stock and replenishment" dependence from the thickening of points on the graphs. The shape of the curve can be estimated in a specific case when the observed population gradually degraded under the influence of fishing. If the fishery has brought the population out of a stable regime and the impact of the catch has long prevailed over the natural dependence in the restoration of the stock; then, due to the consistent reduction of the stock, it is possible to judge the shape of the curve (or the absence of an obvious dependence) on the graph of monitoring data on the number of juveniles, using the moving average method. It was possible to confirm the presence of extremes in the dependence on the graph in the coordinates "stock × replenishment" in such populations [53]. Correlation methods cannot be reliable in this task. A remarkable example of false explicit correlation in the trends of population phenomena was shown [54]. There was no obvious dependence "stock × replenishment" even with the small size of the Kamchatka crab population of the Kodiak archipelago [55]. However, dynamics sometimes allows us to solve the inverse problem and assume the behavior of the system under study.

THE FORMAT OF EVENTS AND TIME FRAMES IN THE REPRODUCTION MODEL

We are not just developing another model function "stock-replenishment"; we will describe a methodology for representing functional dependence for scenario analysis of situations with nonlinear effects that we need for this task.

It is often necessary to introduce additional conditions into ecological models both for the beginning and for the completion of the factor, since the course of processes can change abruptly when a number of conditions in the environment are met. "Hybridity" has now become too broad a term in modeling (meaning pulse, automatic, etc.) [56]. The author of [56] developed variously recorded dynamic models that relate to hybrid structures and differ in the type of switching organization. We define the chosen construction as a predicatively redefined computational structure with a frame-by-event time and use the methods of glued calculations.

It is important for the methodology to adapt the representation of model time as a sequence of tuples of events and to determine the logic of switching. The points in the cropped continuous time for events that lead to rearrangements in the system of differential equations can be determined by probabilistic or logical methods. Events are required to describe structural qualitative changes as special states in the space of variables with zero duration.

The life cycle of the standard length of an aquatic organism developing from eggs (both fish and crustaceans) before puberty is accompanied by metamorphosis. The sequence of continuous time intervals connected by the algorithm can be biologically justified using the ideas of the theory of the phasing of the development of hydrobionts, developed by the scientific school of B.B. Vasnetsov [57, 58]. For each species, there are significant metamorphoses in the ecologo-physiological development that change its role in the trophic chain of the community and survival; therefore we will set the division of the vulnerability interval into stages. The change in the survival rate by 1% at the stages in early ontogenesis is of great importance. In tasks with switching, it is logical to set the time format with a continuous and with a discrete component. For this task, we will choose a format that is suitable for modeling a process with a modified impact and especially in a situation of expert fishing management.

We use framing of the hierarchy of continuous time intervals in computational experiments with a predicatively variable form of impact. Inside the main frames, we will make an order of numbered events t^i. Hybrid event time for computational experiments is formalized in the form of a multiset of ordered elements on a fixed interval length T:

$$\bigcup_n \left\{ \uparrow L_n, \left\{ \bigcup_i [t_0, t^i, t^{i+1}, T] \right\}_n, \downarrow, R_n \right\},$$

where i is the number for the event inside the frames before T and n is the current frame number in the order of successive generations. Recording time with two discrete components leaves the edges $\{\uparrow L, \downarrow R\}$ to the right and left of the main unit, the frame with the number n. The edges between time frames that are not included in the frame in the form of points $\{\uparrow L, \downarrow R\}$ are needed to perform rebuilds in the points of system transitions that are highlighted by the conditions. At the right point $\downarrow R$, the settings of the magnitude of the impact of fishing are changed. At the left point $\uparrow L$ we make the transition to the calculation of the development of the next adjacent generation. The purpose of time formalization is to accurately introduce elements of eventfulness in management, since the points t^1, t^2, and t^i will be indicated from calculations of completely continuous additional variables. It is not always necessary to format time with floating-length subintervals into fixed frames due to calculated events. Eventfulness can be entered without setting a frame, as in physical tasks with relay switching.

The idea of time manipulation is that the computational model of a generation's life is formed based on a dynamically redefined system. The factors of population decline vary significantly between the stages of ontogenesis and development of crustaceans [59].

BASIC PREDICATIVE COMPUTING STRUCTURE

The changes represented in the model by their essential genesis are strictly mandatory, algorithmically predetermined in time, or optional consequences of other processes. The choice of an alternative equation in the model is carried out only with a special ratio of the calculated values. The second idea of the method, which can be applied to different populations, is to determine events from the assessment of the state of the set of predicates, followed by changes in the procedure for calculating equations. For a model reflecting biological discontinuity, we propose a computational structure with sequential redefined forms that preserve continuity. The value of $N(t)$ in each frame changes from $N(0) = \lambda S$ to $N(T)$, where λ is the average fertility for the five previous seasons. The system is formalized by a differential equation with a set of possible "interchangeable forms" for the right side and additionally with a set of predicates for changing the calculation mode, Boolean functions $P(x, y)$ with a set of values {0;1}. The predicate is given by the mathematical relation of continuously changing arguments. Predicates are by default at t_0 $P(x, y) = 1$, and they will necessarily have to take the value $P(x, y) = 0$ from the state of their arguments at t^i (or vice versa, change the value from 0). The arguments $P(x, y, ...)$ in our method are variables from auxiliary and related to the dynamics of $N(t)$ equations, calculated synchronously with equations (2).

The time of ontogenesis before entering the reproductive age of successive generations is set by combining time intervals with a set of calculated events:

$$t \in [0, T] \equiv \bigcup_i \{[t_0, t^i, t^{i+1}, T]\}. \quad i = 1...3.$$

Biologically, the frame interval is the standard lifetime of a generation before the start of reproductive activity. Numbered event points in the interval of juvenile ontogenesis are ontogenetic "interruptions". Compare these metamorphoses with the equations in the right part for the decrease in the number of the

generation from $N(0)$, which is uneven at the three main stages of early ontogenetic development:

$$\frac{dN}{dt} = \begin{cases} -(\alpha_1 w(t)N(t) + \beta)N(t),\ P_1()t \\ -\alpha_2 N(t)/w(\tau) - \beta N(t),\ P_2(t, w(t)) \\ -\alpha_3 w(t-\xi)N(t-\xi) - \beta,\ P_3(t, w(t)). \end{cases} \quad (2)$$

The parameters $\alpha_1 < \alpha_2 < \alpha_3$ and β are the coefficients of juvenile mortality depending on the number of the generation itself. The third in order of equations (2) with α_3 a small delay $\xi < \tau$ is included to account for the exhaustion of resources by early stages, where τ is the length of the earliest stage. For the second stage prone to predation, the growth factor $w(\tau)$ reduces the loss. The predicates P_1, P_2 and P_3 give biologically interpreted moments when to stop calculations of each of the forms of the right part, the condition for completing the activity of the equation and obtaining intermediate results:

$$P_1(\neg t < \tau), \quad P_2(t \geq \tau, t \neq T, \neg w_t < w_k), \quad P_3(t = T, w_t < w_k). \quad (2.1)$$

We have written two predicates in expressions (2.1) with logical negation, so these events will become possible if the relations are violated. The calculation of equations (2) considering the conditions (2.1) occurs with the cycle algorithm until $P_i = 1$. Predicates must always define transition events in the time frame uniquely and for each t. Avoiding ambiguity, we can additionally use logical variables, flags that change the state from one to zero if the transition is prohibited. Recording a continuous-event model time as a multiset of $\langle t_0, t^i, t^{i+1} \rangle$ elements means that the model considers a sequence of frames for the life cycle time of an individual generation. Inside each time frame with the initial position t_0 there are "intra-frame" events, which we have designated by the superscript t^i. The transitional level of development w_k was used to exit the generation from a quadratically determined mortality rate. The set of events can be expanded. For each form of the right part, at the moment of the event, the initial conditions associated with the previous calculations are calculated. To calculate the dynamics of the new $(n + 1)$ generation, the initial conditions for the first in the structure of equation (2) are reinitialized:

$$N(0)_{n+1} = \lambda S_n, S_n = \left(N(T)_n + \sum_{m=1}^{k} \nu_m N(T)_{n-m} \right),$$

where ν_m is the indicator of post-spawning survival for a series of previous m generations, and S is the number of the stock ready for reproduction with average fertility λ.

Population processes are variable even without the influence of fishing. In the scenario application of the model, it is important to estimate the current values of the P_1, P_2, P_3 set. Transitions of two types in equations (2) are recorded, that is, only those based on the counts of time unit segments t and caused by internal ratios of the calculated indicators. In this case, the shape change in equations (2) occurs after comparing the ratios of values under conditions (2.1) for internal model variables, by $w(t)$; however, another species-specific dynamic characteristic can be used. The idea of using related characteristics and calculations of auxiliary indicators makes it possible to expand the basic model in a variety of ways. Fishery management is represented by a special scenario algorithm in a hybrid model. It is convenient to vary such a control effect according to the given logic of the scenario with the eventfulness of the computational experiment.

We use the interdependence often noted in many species [60] between the growth rates of juvenile aquatic organisms and mortality, which was proposed to be used for modeling in [61] with the inverse dependence $w'(t) = l(N^{-1}(t))$. The predicative structure of the set of right-hand sides of equation (3) will be solved numerically in relation to the auxiliary indicator of the average dimensional development of individuals of the generation $w(t)$:

$$\frac{dw}{dt} = \frac{\sigma}{\sqrt[3]{(N(t) + \delta)^2}} + \chi_C, \quad (3)$$

where δ is a corrective indicator, and σ is a fixed reflection of the abundance of food resources, which can also be a seasonal periodic dependence $\sigma(t)$. The energy spent on growth in hydrobionts in northern latitudes depends on temperature [62]. Here $\chi_C \in [-\varepsilon, \varepsilon]$ is a correction related to temperature, it can be positive or negative. For optimal spawning conditions in equation (3) we take $\chi_C = 0$. Thus, the availability of an available food supply affects survival in the model indirectly.

We will calculate $R = N(T) = \varphi(N(0))$ to determine the properties of the phase portrait of iterations $R_{n+1} = \varphi(R_n)$. We are interested in the boundaries of the field of attraction and singular points.

SMOOTHLY TRANSFORMABLE MODEL DEPENDENCE

It is necessary to reflect the effect of the aggregated group [63], since we are considering situations for populations outside the historically established number. With a small number of S, the role of unfavorable factors in reproduction is high [64, 65]. It is methodically wrong to introduce an explicit minimum L threshold of the Ollie effect here, as in the Bazykin equation [66]. The L threshold is unknown to experts in advance, and not all changes in regulation are rigidly predetermined. According to ecological criteria, changing the basic population characteristics by a leap is unreliable.

We have developed a method for taking into account the variability of factors in the form of a point

introduction into a predicatively redefined dynamic system of special functions as varying coefficients, $\Psi(n) \neq \text{const}$ for iterations of $\varphi^n(x_{n-1}, \Psi(n))$, with only a limited range of values. Such functions should be constant throughout the frame $[\uparrow L, \downarrow R]$ of continuous model time. Triggers in calculations will change their function value when the frame $n := n + 1$ is changed. Ψ is associated with the initial state.

In the equation of the decrease in the number of generations, the mortality coefficients are divided to αN^2 and βN. The value of $w(t)$ with the parameter α_i takes into account the rapid depletion of resources necessary for development as the total biomass of larvae increases. It is important to consider the loss of reproduction at the stage with t_0. The effect of losses can be strongly manifested at a low density of mature individuals $S \to \min\varphi$, more eggs will remain unfertilized. The effect of the reproduction efficiency reduction for a small group is realized in the model by a dynamic coefficient with βN. Its influence depends on the size of the parent population S, from which we calculated the initial conditions $f(S)$. The range of influence of $N(0)$ on Ψ should be limited. The range of values of the "trigger function" $f(S)$ on the right has a quickly achievable end limit:

$$\Psi(S) = 1 + \exp(-\zeta\sqrt[3]{S^2} + \varepsilon),$$
$$\lim_{S\to\infty} \Psi(S) = 1, \Psi(0) = 2.$$

The $\zeta(\zeta < 1)$ coefficient will reflect the level of expressiveness of the effect of losses from the original roe. With an optimal stock, Ψ does not determine the calculations, which will allow the factor to be turned off smoothly in equation (2) for the first stage:

$$\frac{dN}{dt} = -\alpha w(t) N^2(t) - \Psi[S]\beta N(t). \qquad (4)$$

In equation (4), we took into account smooth changes in regulation, whereas in the hybrid system we described threshold changes in the dynamics of the decline in the number of juveniles, which cannot be avoided. The structure of the hybrid model in the Rand Model Designer computing environment can be adapted for a group of co-living and competing generations.

A METHOD FOR ANALYZING DISCRETE ITERATIONS OF A HYBRID MODEL

By obtaining with $N(0) \to N(T) \equiv \varphi(N(0))$ the functional dependence after numerically solving equations (2) and (2.1) together with (3) and (4) and with $N(0) = \lambda S$ for biologically acceptable values of $N(0) \in \mathbb{N}$, it is possible to evaluate the dynamic properties of the iterations $\varphi(\ldots\varphi(x_0))$ of this dependence. The numerical solution with the calculation of $N(T)$ is used to calculate the functional iterations $R_{n+1} = \varphi(R_n) - q_n R_n$, where the coefficient $q \in [0,1)$ is the established share of commercial seizure. With regulated fishing, q is set by experts for each season n, which will be considered in the scenario study of the development of the situation. The most important parameter of the model for changing the form of dependence and the behavior of iterations turns out to be the fecundity of λ, but in ecological reality this is a slowly changing characteristic.

In iterations, we will get the separation of the set of available starting points R_0 of the trajectories of an unstable "repeller" point. So the iterations will get two areas of attraction Ω_1 and Ω_2 for two alternative attractors. The dependence used as the evolution operator φ will have more than one maximum (Fig. 10). For us, the position relative to each other of the first from the origin of the coordinates of the maximum $R_{\max}$ and the local minimum $R_{\min}(R_{\min} > R_{\max})$ is important, but the preservation of $\varphi(R_{\max}) > R_{\min}$ is significant.

We will obtain a family of nonlinear curves relevant to the problem with extremes and horizontal asymptote by changing only the effect of Ψ and not changing the values of the generation loss parameters in equation (2). The mathematical basis for the analysis of their iterations is the theory of the dynamics of maps developed in [67] with the Schwarzian value changing sign when the argument changes. For iterations of the function $x_{n+1} = \varphi(x)$ with three extremes, the conditions of the D. Singer theorem [68] are not satisfied, which are necessary for the realization of the scenario of the transition to a global chaotic attractor through a cascade of bifurcations of doubling the period of the cycle $p \to \infty$ according to the Feigenbaum-Collet-Tresser theory [69], since with a smooth change in the parameter of such an iteration $x_{n+1} = \varphi(x)$, two alternative stable cycles of an even period ($p = 2$) will arise. Accordingly, the cascade will not be infinite and the Cantor set will not be formed.

The arsenal of descriptive tools for iteration dynamics is wide, although limited [70]. Three topological forms of attractors are available for $R_{n+1} = \varphi(R_n)$ iterations, namely, a finite period cycle or an equilibrium point $x^* = \varphi(x^*)$, an attractor similar to a Cantor set, and an interval attractor in the form of a conjugation of an uncountable set of segments. For iterations $x_n = \varphi(x_{n-1}) \pm \Theta(n)$ (taking into account the changing external perturbation), there are three types of bifurcations, rearrangements of the type and number of attractors, which are direct and inverse. Attractors other than equilibrium points can instantly lose the invariance property $f(\Lambda) \in \Lambda$, which depends on the position of the boundary $\partial\Omega$ in their region of attraction Ω. The attractor can break into parts or intersect with the boundary of its area of attraction Ω: $\forall x_0 \in \Omega$ and $\lim_{n\to\infty} \varphi^n(x_0)$, and at this moment a cri-

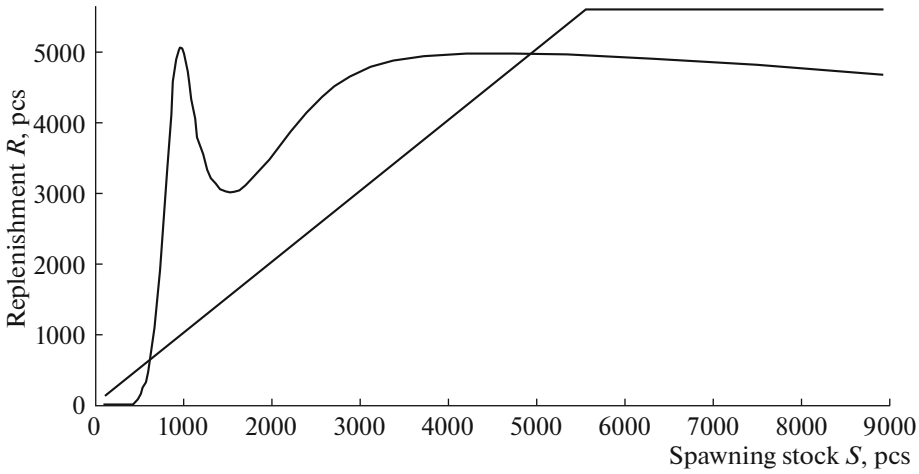

Fig. 10. A graph of the model dependence with three extremes and two equilibria at the points of intersection with the bisector of the coordinate angle.

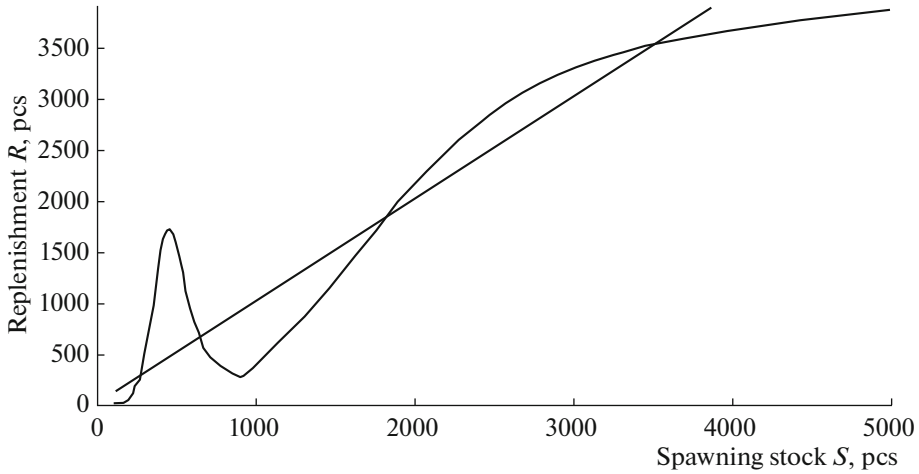

Fig. 11. The model dependence with nontrivial equilibria and intersections with the bisector of the coordinate angle at $\min \varphi(S) < R_2^*$, $\max \varphi(S) > R_3^*$.

sis situation is fixed. So the theory of maps intersected with the problem of biocybernetics.

ANALYSIS OF A NONLINEAR COLLAPSE SCENARIO

Scenario modeling that allows to comparison and evaluation of variants of situations is an approach to the regulation of multi-species fishing [71]. Consider the dynamics of collapse in a scenario experiment with the logic of expert management of commercial seizure. The mathematical basis of the scenario will be the metamorphoses of the phase portrait of iterations caused by the transformation of the extremes of the dependence. In the scenario model, it is better to calculate the number of individuals Y_n withdrawn from the stock S in the fishing season n instead of the mass, which will be the observed value.

For our problem, we obtain the dependence when solving three Cauchy problems glued by $N(0)_i$ from equation (2) with a non-constant number of nontrivial stationary ($\varphi(R_i^*) = R_i^*$) states due to the level of external influence q; however, their number should remain at least two for each n. In the initial situation, the curve $\varphi(S)$ without significant impact is characterized by four increasing points $0 < R_1^* < R_2^* < R_3^* < R_4^*$, equilibrium states (Fig. 11) (the position of the graph of the model dependence relative to the coordinate angle bisector) that do not coincide with the extremes of the curve. The dependence with a pronounced minimum was determined earlier for the Volga starry sturgeon [72].

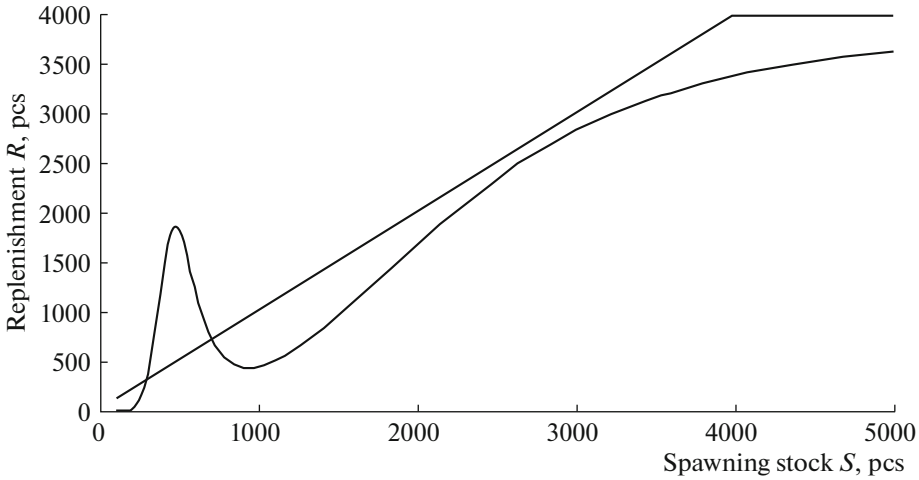

Fig. 12. The curve of the model dependence after the inverse tangent bifurcation with two unstable equilibria and $\min \varphi(S) > R_2^*$.

For the targeted reconstruction of the phase portrait in the scenario, three unstable stationary points are needed with stability $R = 0$ for each n. The first metamorphosis will be obtained by gradually increasing q, which will cause an inverse tangent bifurcation, the fusion of a stable R_4^* with an unstable R_3^* equilibrium. As a result, we observe the loss of the largest equilibrium state, the previously attracting point of the trajectory for the Ω_2 region (Fig. 12).

The structure of the hybrid system of equations makes it possible to scale the evolution operator φ along the abscissa axis in computational scenarios and change the positions of the extremes φ according to the influence of external conditions. The function Ψ does not change the relative position of the fourth stable equilibrium R_4^*, but affects the position of $\min\varphi(S)$ relative to the precritical unstable repeller R_2^*. R_1^* plays the role of a critical repeller and the boundaries of the areas of attraction $\partial\Omega$. The projections of the extremum points of the local maximum and minimum have an important property, namely, the maximum is displayed by the abscissa to the right of the minimum ($\varphi(R_{\max}) > R_{\min}$). It is possible to transform extremes and nontrivial equilibria at $\varphi(\lambda S)$ from $\min \varphi(S) < R_2^*$ and $\max \varphi(S) > R_3^*$ into the form of $\min \varphi(S) > R_2^*$ and $\max \varphi(S) > R_4^* > R_3^*$. Changes in these ratios in the dependencies $\min \varphi(S)$ dramatically affect the qualitative behavior of the iteration trajectory.

A set of parameters of a computational experiment for a situation when a commercial crab population has recovered to a stable equilibrium optimal for its food base after an unstable existence can be made. The basis for the assessment will be a model season of 12 model months. Crab catches $Y_n = R_n q_n$ are gradually increasing without forcing the fishery. After spontaneous growth, experts make a decision based on their logic to raise the annual quota ($\overline{q}_n = 0.62$). It is quite logical that crab catches for the first four seasons after the increase in the share of seizures show historically record values for the fishery ($Y \to \max$). After "successful" seasons, catches sharply drop. The volumes of commercial crab stocks bypass the local minimum of the reproduction curve φ, avoiding falling into the ε neighborhood of the critical state R_1^*. Experts see stabilization, as they are used to averaging Y_n. According the logic of expert forecasts, in this scenario, good reproduction efficiency for previous seasons was taken into account immediately after the loss of equilibrium and the passage of a local minimum ($q = 0.35$) was established. Catches after the first fall began to increase significantly. According to the statistical methodology, experts have no reason to adjust fishing management for further decline.

The value of the reserve after the increase in fishing pressure breaks into the aperiodic mode, but in a limited range of values. As a result, the time of the catch growth Y after the minimum is unpredictable. Experts will see changes similar to fluctuations caused by the instability of environmental conditions. The decision to minimize the withdrawal rate to $q = 0.2$ in the oscillation mode is rejected. When $q > 0.33$ is set, after the trajectory passes through the neighborhood of R_1^*, a population collapse is realized in the computational scenario (Fig. 13). Fishing stops, although the catch quota for the season has been allocated, as it happened with cod in 1992.

The final drop in catches was called the "collapse", while the first reduction in crab catches was thought temporary and barely noticed, in absolute terms it was greater. During the first crisis, crab catches decreased sharply, which did not entail a seasonal full moratorium on fishing. Fishing was continued under unstable fluctuations with constant fishing pressure and a moderately favorable forecast. According to the prin-

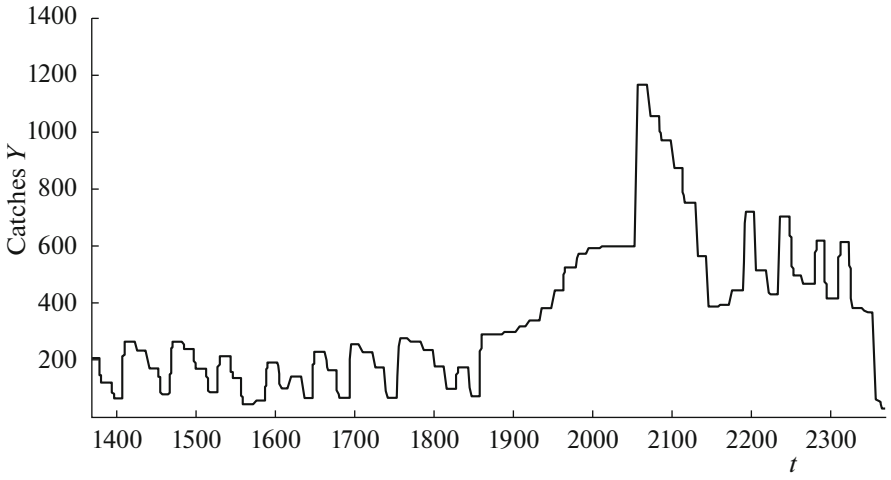

Fig. 13. The computational scenario of catch dynamics with the effect of stock collapse.

ciples of nonlinear dynamics, this behavior is regarded as a sign of the presence of critical points; however statistical methods cannot establish points for the stock when the function connecting the stock and replenishment changes almost vertically.

Modeling has shown that the path to the final crisis consists of transitional regimes. In a computational experiment, the scenario of collapse of Kamchatka crab commercial stocks develops from two phases; their duration depends on the increase in Δq with the intensification of marine fishing. If a timely moratorium has not been introduced, the second phase of degradation will inevitably occur after eleven model seasons in the time format of the computing environment with the transition through the threshold of critical unstable equilibrium. In the model, the reproduction of the population after the degradation phase does not compensate for the natural decline of parental generations; therefore, the introduction of adult crabs from other places is necessary.

PHASE PORTRAITS OF THE COLLAPSE SCENARIO WITH OSCILLATIONS

Three nonlinear phenomena called "crises" are known for functional iterations [73]. In addition to the basin-boundary crisis, an internal crisis and a merging crisis are identified; the latter is specific to the scenario of doubling the cycle period ($p = 2^i, i \to \infty$) [74]. Crises are not caused by transformations of the topological types of the attractors and bifurcations themselves; they are associated with rearrangements of the position of the attractor relative to its neighboring unstable invariant sets, a single point or a fractal set.

The phase portrait metamorphosis used in the scenario is the boundary crisis of the interval attractor Λ, which remains after the merger of stable and unstable equilibria. In the order of the list of Huckenheimer's theorem [75], this topological type of closed ω-limit sets of iterations is No. 3 of the three possible types of attractors. The effect of the crisis occurs when Λ comes into contact with the boundary of its area of attraction. Initially, the neighborhood of the local maximum, where the value of Λ slightly exceeds the value of φ at the point of the third repeller, is $\varphi(\max \varphi(N(0)) \pm \varepsilon) > R_3^*$. When tangent bifurcation occurs, the unstable and stable points R_3^* and R_4^* merge into one critical point R_C^* ($\varphi(R_C^*)) = 1$), which disappears. This is how we simulate the first drop in the crab catch. The stability of the iteration point $\varphi(R^*) = R^*$ can be estimated by the position of the tangent from the known property $|\varphi'(T^*)| < 1$. We denote the cumulative set of prototype points of the second repeller R_2^* as $\{\varphi^{-n}(R_2^*)\}$, and the inverse iteration of the function φ into the right prototype of the point R_2^* as $\varphi^{-1}(R_2^*) = R_2^{-1*r}$. These prototypes are excluded from the field of attraction; they are never attracted to the attractors. If there are direct prototypes for R_2^* both to the right and to the left of the point, this will make Ω_2-the area of the attraction of R_4^* disconnected. The repeller R_2^* exists in all model scenarios and has prototypes both on the right and on the left for each n. The points R_3^* and R_4^* appear/disappear after a forward/backward tangent bifurcation. The equilibrium R_1^* for φ exists for each n; while the presence of a prototype in the repeller R_1^* depends on the values of Ψ increasing as $R_{n+1}^* \to R_1^*$ approaches. When the initial position of the R_0 point of the trajectory turns out to be $R_1^* < R_0 < R_2^* < R_3^*$ and corresponds to a subset from the $R_0 \in (R_1^*, R_3^*) \cap \{\varphi^{-n}(R_2^*)\}$ interval, the population in the scenario will reach the level of high stable abundance in a finite number of steps $\varphi^{\vartheta}(R_0) = R_4^*$, $\vartheta < \infty$ through the mode of

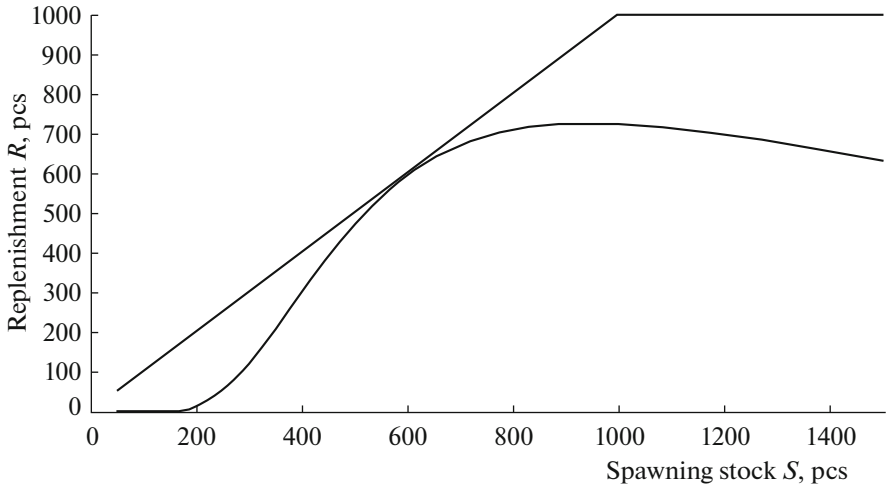

Fig. 14. The transformation of unimodal model dependence after one tangent bifurcation.

pseudo-stochastic fluctuations. Therefore, the scenario of population recovery with a timely moratorium and $q = 0$ in the model is real, $0 < R_0 < R_2^*$, $\lim_{n\to u} \varphi^n(R_0) = R_4^*$; a boundary crisis is possible even when in contact with R_3^*.

It is assumed that for finite-dimensional smooth dynamical systems we can observe three fundamentally different forms of chaos [76]. The characteristics of irregular fluctuations of points generated by our $\varphi^n(R_0)$ are a consequence of the shape of the curve with three extremes and the instability property of the intermediate results obtained during calculations at different positions of the initial point of the trajectory R_0. This is due to the "riddling" region I in the phase space. The phenomenon of riddling occurs when nested invariant sets are formed [77]. Segment I includes a scattered continuum set of subintervals from the regions of attraction of Ω_1, Ω_2 of two attractors. The boundaries of all subintervals do not belong to these regions of attraction and form a separate set, the "strange repeller", which is an invariant closed set, in any ε-neighborhood of which there are points belonging to the region Ω_1, Ω_2. The boundaries of the "riddled" region I will determine the maps of the points $R_{\min} > R_{\max}$, so that $I = [\varphi(R_{\min}), \varphi(R_{\max})]$ for two extremes of the model dependence, but not the fixed interval $[R_1^*, R_3^*]$, since the very existence of R_3^* depends on q_n. The starting points $R_0 \in [\varphi(R_{\min}), \varphi(R_{\max})]$, which can be attracted to the attractor, are everywhere adjacent to those that are never attracted to R_4^*. Combinations of sets of those points R_0 that are mapped to unstable repeller equilibrium positions under the action of iterations of φ are excluded from the interval I. When unstable stationary points on the graph of the replenishment efficiency dependence φ have more than one direct prototype, the point R_2^{-1*}, which will be displayed in the repeller $\varphi(R_2^{-1*}) = R_2^*$ at the first iteration, the aperiodic mode observed in computational scenarios, and uncertainty of the trajectory behavior arise due to the riddling of I.

The interval I between the displays of the extremes of the function φ will include the interval attractor $\Lambda \subset [\varphi(R_{\min}), \varphi(R_{\max})]$ within itself. The interval I contains an attractor of the interval type $\Lambda \subset I$, where Λ is a closed invariant subset of I, but Λ is disconnected, since any ε neighborhood of a point $\forall R_0 \in \Lambda$ contains non-stretching points from an invariant and continuum set Υ, minimally consisting of all R_2^* prototypes and having both right and left direct prototypes, $\{\varphi^{-n}(R_2^{-1*r}), \varphi^{-n}(R_2^{-1*l})\}$. A subset of the strange repeller will make up the entire union of points R_0 scattered in I without attraction:

$$\Upsilon = \bigcup_n^{\infty} \varphi^{-n}(R_2^*), \varphi^{-n}(R_1^*), \varphi^{-n}(R_3^*).$$

The trajectories of the starting point $\{\varphi^n(R_0)\}$, $R_0 \notin \{\varphi^{-n}(R_2^*)\}$ have the possibility of falling into the ε neighborhood of the chaotic repeller Υ, consisting of a set of all non-stretchable points and arising when the position of the extremes of the dependence $\varphi(R)$ changes. When the conditions $\exists R_0$, $R_0 \in I$, $R_0 \notin \Upsilon$ and $\varphi(R_0) < R_1^*$ are met, the intervals in Λ will no longer be a closed and invariant subset where the condition $\varphi(\Lambda) \in \Lambda$ is met. Chaotic movement in a finite number of iterations φ^k, $0 < k < \infty$ is observed in I with the end of the chaotic mode $\lim_{n\to d} \varphi^n(R_0) = 0$, $k < d < \infty$. The duration of the aperiodic modes varies somewhat due to the sensitivity to perturbations of the $R_0 \pm \varepsilon$ at the time point, which we choose as the initial point in the computational experiment. The property

of randomization, limited both in time and in the range of I values of $\varphi(R)$, reflects the natural uncertainty for a marine fishing object.

We noted that other collapse scenarios can develop without fluctuations. For such situations, a less complex dependence can be obtained in the model, initially having a pair of stationary points. Stable and unstable points begin to merge into a critical equilibrium, as in Fig. 14. At this moment, the trajectory stabilizes up to the disappearance of the only stationary point R_C^*.

This variant of collapse is mathematically described more simply, without complex transient modes, and requires a single metamorphosis of the phase portrait. In a state of dependence $\forall 0 < R$, $R \neq R_C^* \varphi(R) < R$, a small unpredictable external pressure and an increase in natural mortality can lead the population to collapse.

CONCLUSIONS

A variant of the degradation of commercial stocks after finding the population in a state of unstable oscillations has been considered. A method of mathematical formalization of non-trivially varying reproduction efficiency in the traditional form of dependence of stock and received replenishment has been developed. A computational scenario with the implementation of two metamorphoses in the phase portrait of an iterative dynamic system to account for the identified features of the degradation of commercial crab stocks is presented. The collapse scenario in the model confirmed that the ideas for organizing the optimal, most profitable strategy for the exploitation of biological resources are dangerous in reality. The optimal state for fishing is close to the critical threshold, where there is a high probability that reproduction ceases to replenish the stock. The randomization in the new hybrid model successfully simulates stochastic perturbation of the conditions of the breeding environment.

The Canadian cod crisis has been thoroughly examined; however, its key cause has not been established. The collapse of the Kamchatka crab, as well as cod off the coast of Labrador, was provoked by distorted ideas about the well-being of these biological resources and, most importantly, by overestimating the effectiveness of replenishment of reserves. The real dependence on the intensification of fishing lay closer to the bisector $R=S$ than experts assumed. The reason for the overestimation error was that the extremes of the non-monotonic dependence shift as the stock number depletes in the range of $S \in [\varphi(R_{\min}), \varphi(R_{\max})]$ values. With intensive fishing, the value of $\varphi(R)$ at the extremum of $R_{\min}$ is shifted downwards along the ordinate axis in such a way that $\varphi(R_{\min}) < R_1^*$. Next, a boundary crisis is realized for the Λ attractor, composed of a set of intervals $\exists y \in \Lambda$ and $\varphi(y) \notin \Lambda$. After the crisis, the points of the trajectory $\exists x_{0i} \in \Lambda$, $\lim_{n\to\infty} \varphi^n(x_{0i}) = 0$ appear. The point R_1^* is an unstable equilibrium for the population at a critical number; if $\varphi(R_{n+1}) < R_1^*$, irreversible degradation of the stock is realized for a finite number of iterations $\varphi^k(R_n) = 0$. The final collapse is reflected in the simple form $R_0 \notin \Upsilon, \varphi^k(R_n) \to 0, k < \infty$. In the $S \in (R_2^*, R_2^*)$ range, the reproduction efficiency according to our model is still quite high due to the local maximum. This introduces misleading expectations of the continuation of the trend of reproduction recovery. It has been shown that with a further small loss of the stock, the reproduction efficiency in the disproportionately sharply decreases until the critical threshold of replenishment of stocks is almost reached.

A small systematic error in stock estimates in the $S \in (R_2^*, R_2^*)$ range is sufficient for the collapse of the fishery, since the actual share of withdrawal will be higher than planned; moreover, this discrepancy will increase over time. After the first drop in the population, there is a sharp transition to a state of strong irregular fluctuations with pronounced local peaks, but this is still a reversible state. The population will be able to recover if an unobvious management decision is taken immediately and the withdrawal is halved.

We consider limitation of the technical capabilities for fishing (the size of fishing gear, the fuel supply on ships, and the tonnage of ships) to be a rational tactic when regulating catch, but not a limit on the volume of production: strict quotas do not save populations. Paradoxically, it's time to figure out how to temporarily reduce the effectiveness of fishing gear on complex fishing objects. Registration of a 20% reduction in catches for non-cyclical populations of large dominant predators is the basis for the introduction of a seasonal moratorium on catch. The fishery should not be motivated to underestimate the actual catches in reporting. Monitoring data on the survival of juveniles is necessary for the exact choice of the permissible level of exploitation, which was obtained during observations of the spawning of the Volga starry sturgeon [78, 79]; however, they were evaluated after degradation.

The originality of the hybrid modeling method with the inclusion of event changes comprises the analysis of the ways of development of the existing situations. The phenomenon of collapse develops according to the internal logic of the traditional method of expert fisheries management for many countries when issuing seasonal quotas [80] based on estimates using statistical smoothing and approximation of the number of distributed populations of aquatic organisms over a large water area [81]. The use of the developed computational structure is promising as a unit of reproduction calculations as part of modern multi-species models of biosystems [82]. The dif-

ficulty in using aggregated polymodel complexes for forecasting and optimizing fishing is the complex parameterization and interpretation of the results, wherein a small perturbation of one of the many bifurcation parameters will qualitatively change the behavior of the final solution, while a change in the values of other coefficients will not cause a significant response. The structure can include a stochastic component for individual situations [83].

Examples of crises and rapid outbreaks of different populations require an expansion of the representation of dynamic models for ecological problems. The similarity of the situations confirms our hypothesis about the existence of a finite set of forms of scenarios for the development of extreme changes in ecodynamics. In this case we will be able to classify (regardless of their nature) the forms of changing processes known to us (outbreaks, crises, and formation and destruction of irregular oscillations with a large amplitude), by comparing them with the known types of metamorphoses as a set of tools (bifurcations of attractors or rearrangements of the boundaries of their areas of attraction) of phase portraits of discrete or continuous dynamical systems for describing scenarios. The commonality of nonlinearity and the typification of scenarios create a functional of regulation. The concept of dynamic collapse was applied in [84] not only to individual populations, but also to entire biocenoses.

Close attention should be paid to the mathematical description of threshold states and rapid transformations when forecasting processes with nonlinear regulation [85], which is relevant now, for example, for age-related changes in the effectiveness of the adaptive immune system, noted in [86]. Synthetic "polymutant" pseudotypes of the *S*-protein were generated to select the optimal antigenic target and predict the further evolution of SARSCoV-2 strains; it was shown, in particular, that the ability to neutralize antibodies previously developed in patients infected with the original virus variant decreased with the accumulation of *S*-protein mutations sharply and in a threshold manner [87].

COMPLIANCE WITH ETHICAL STANDARDS

Conflict of interest. The author declares that she has no conflicts of interest.

Statement on the welfare of humans or animals. This article does not contain any studies involving animals performed by the author.

REFERENCES

1. A. Yu. Perevaryukha, Biophysics (Moscow) **66**, 974 (2021).
2. A. Yu. Perevaryukha, Biophysics (Moscow) **65**, 118 (2020).
3. L. Loyal, J. Braun, L. Henze, et al., Science, **374**, eabh1823 (2021). https://doi.org/10.1126/science.abh1823
4. L. R. Clark, Aust. J. Zool. **12**, 362 (1964).
5. R. ud Dina, A. R. Seadawyb, and K. Shah, Results Phys. **19**, 103468 (2020).
6. A. M. Syed, T. Y. Taha, T. Tabata, et al., Science, **374**, 1626 (2021). https://doi.org/10.1126/science.abl6184
7. Yu. D. Nechipurenko, A. A. Anashkina, and O. V. Matveeva, Biophysics (Moscow) **65**, 703 (2020).
8. T. A. Zaichuk, Yu. D. Nechipurenko, A. A. Adzhubey, S. B. Onikienko, et al., Mol. Biol. (Moscow) **54**, 812 (2020).
9. T. Maemura, M. Kuroda, T. Armbrust, et al., mBio **12**, e01987-21 (2021). https://doi.org/10.1128/mBio.01987-21
10. A. F. Vanin, A. V. Pekshev, A. B. Vagapov, et al., Biophysics (Moscow) **66**, 155 (2021).
11. A. F. Vanin, Biophysics (Moscow) **65**, 698 (2020).
12. A. R. Kathryn, R. K. Bewley, and S. A. Fotheringham, Nat. Commun. **12**, 81 (2021).
13. A. Yu. Perevaryukha, Biophysics (Moscow) **66**, 327 (2021).
14. W. van Damme, R. Dahake, and R. van de Pas, Med. Hypotheses **146**, 110 (2021).
15. T. I. Kornilova, Rybovod. Rybn. Khoz., No. 8, 34 (2011).
16. N. I. Reus and S. V. Petrova, Arktika: Obshch. Ekon. **8**, 115 (2012).
17. Order of the Federal Agency for Fisheries No. 443 of December 19, 2006. https://www.garant.ru/products/ipo/prime/doc/2067316/.
18. G. I. Guteneva, S. S. Fomin, and T. N. Dedikova, Rybn. Khoz., No. 3, 103 (2015).
19. G. P. Ruban, R. P. Khodorevskaya, and V. N. Koshelev, Astrakhan. Vestn. Ekol. Obraz., No. 1, 42 (2015).
20. T. Yu. Borisova, Candidate's Dissertation in Biology (Astrakhan, 2010).
21. T. N. Solovieva, Inf.-Upr. Sist., No. 6, 58 (2017).
22. T. N. Solovieva, Inf.-Upr. Sist., No. 4, 60 (2016).
23. P. V. Veshchev, G. I. Guteneva, and R. S. Mukhanova, Russ. J. Ecol. **43**, 142 (2012).
24. A. Yu. Perevaryukha, Ekol. Sist. Pribory, No. 8, 41 (2008).
25. A. Yu. Perevaryukha, Nelineinyi Mir **10**, 255 (2012).
26. Yu. V. Tyutyunov, I. N. Senina, L. I. Titova, L. V. Dashkevich, Biophysics (Moscow) **65**, 338 (2020).
27. A. V. Nikitina, A. I. Sukhinov, G. A. Ugolnitsky, et al., Math. Model. Comput. Simul. **9**, 101 (2017).
28. K. Aagaard and J. L. Lockwood, Biol. Invasions **18**, 1667 (2016).
29. A. S. MacDougall, K. S. McCann, and G. Gellner, Nature **494**, 86 (2013).
30. K. Kleisner and D. Pauly, in *The State of Biodiversity and Fisheries in Regional Seas*, Fisheries Centre Research Reports, Ed. by V. Christensen, S. Lai, and M. Palomares (Univ. of British Columbia, Vancouver, 2011), pp. 37–40.

31. A. May, Newfoundland Q. **102**, 41 (2009).
32. J. Roughgarden and F. Smith, Proc. Natl. Acad. Sci. U. S. A. **93**, 5078 (1996).
33. R. A. Myers, Ecol. Appl. **7**, 91 (1997).
34. A. Hutchings and R. A. Myers, Can. J. Fish. Aquat. Sci. **51**, 2126 (1994).
35. Report of the Standing Committee on Fisheries and Oceans. www.ourcommons.ca/Content/Committee/421/FOPO/Reports/RP8826804/foporp10/foporp10-e.pdf.
36. M. G. Karpinsky, *Benthos Ecology in the Central and Southern Caspian S*ea (VNIRO, Moscow, 2002) [in Russian].
37. A. Yu. Perevaryukha, Zh. Obshch. Biol. **81**, 174 (2020).
38. S. Rowe and G. A. Rose, Nature **556**, 436 (2018).
39. A. E. Bobyrev, V. A. Burmensky, E. A. Kriksunov, et al., Biophysics (Moscow) **57**, 115 (2012).
40. A. E. Bobyrev, V. A. Burmensky, E. A. Kriksunov, et al., Biophysics (Moscow) **48**, 245 (2013).
41. V. A. Dubrovskaya, in *Problems of Mechanics and Control: Nonlinear Dynamical Systems* (2016), Vol. 48, p. 74.
42. Yu. I. Zuenko, Izv. TINRO **166**, 103 (2011).
43. B. Dew and R. McConnaughey, Ecol. Appl. **15**, 919 (2005).
44. J. Hoyle, in *Proc. of the Workshop on the Dynamics of Lake Whitefish* (*Coregonus clupeaformis*) in the Great Lakes (2005), pp. 47–61.
45. W. E. Ricker, J. Fish. Res. Board Can. **11**, 559 (1954).
46. R. J. H. Beverton and S. J. Holt, Great Britain Fish Invest. Ser. 2 **19**, 1 (1957).
47. A. I. Mikhailov, A. E. Bobyrev, T. I. Bulgakova, and A. D. Sheremetyev, Zh. Obshch. Biol. **80**, 418 (2019).
48. V. V. Mikhailov and Yu. S. Reshetnikov, Inf.-Upr. Sist. No. 4, 31 (2018).
49. W. De Melo and S. van Strien, Bull. Am. Math. Soc. **18**, 159 (1988).
50. T. Yu. Borisova and I. V. Solovieva, Mat. Mash. Sist. No. 1, 71 (2017).
51. W. E. Ricker, Bull. Fish. Res. Board Can. **1**, 191 (1975).
52. L. A. Zhivotovsky, V. V. Khramtsov, and M. K. Glubokovsky, J. Ichthyol. **36**, 323 (1996).
53. D. K. Kimura, ICES J. Mar. Sci. **44**, 253 (1988).
54. T. Höfer and H. Przyrembel, Paediatr. Perinat. Epidemiol. **18**, 88 (2004).
55. W. R. Bechtol and G. Kruse, Mar. Coast. Fish.: Dyn., Manage., Ecosyst. Sci. **1**, 29 (2009).
56. V. V. Mikhailov, Nelineinyi Mir **16**, 45 (2018).
57. E. F. Eremeeva, in *Theoretical Principles of Fish Breeding* (Nauka, Moscow, 1965), pp. 129–138.
58. V. V. Vasnetsov, in *Essays on General Problems in Ichthyology* (Akad. Nauk SSSR, 1953), pp. 207–217.
59. R. R. Borisov, A. B. Epelbaum, N. V. Kryakhova, et al., Russ. J. Mar. Biol. **33**, 227 (2007).
60. M. V. Churova, O. V. Meshcheryakova, N. N. Nemova, and M. I. Shatunovskii, Biol. Bull. (Moscow) **37**, 236 (2010).
61. E. A. Kriksunov, J. Ichthyol. **35**, 10 (1995).
62. L. I. Karamushko, Usp. Sovrem. Biol. **128**, 180 (2008).
63. Yu. V. Tyutyunov, L. I. Titova, and S. V. Berdnikov, Biophysics (Moscow) **58**, 258 (2013).
64. G. S. Rozenberg, Samarskaya Luka: Probl. Region. Global. Ekol. **29**, 77 (2020).
65. A. Yu. Perevaryukha, Vladikavkaz. Mat. Zh. **21**, 51 (2019).
66. A. D. Bazykin, F. S. Berezovskaya, Probl. Ekol. Monit. Model. Ekosist. **2**, 161 (1979).
67. A. N. Sharkovskii, Dokl. Akad. Nauk SSSR **160**, 1036 (1965).
68. D. Singer, SIAM J. Appl. Math. **35**, 260 (1978).
69. P. Coullet and C. Tresser, J. Phys. Colloq. **539**, 5 (1978).
70. A. Y. Perevaryukha, Biophysics (Moscow) **61**, 334 (2016).
71. T. I. Bulgakova, Rybn. Khoz., No. 5, 70 (2009).
72. V. A. Dubrovskaya, A. Yu. Perevaryukha, and I. V. Trofimova, Zh. Beloruss. Gos. Univ., Ser. Biol., No. 3, 76 (2017).
73. C. Grebogi, E. Ott, and J. A. Yorke, Phys. D (Amsterdam, Neth.) **7**, 181 (1983).
74. B. Reisner, A. Kittel, S. Luck, et al., Z. Naturforsch. **50**, 1105 (1995).
75. J. Guckenheimer, Commun. Math. Phys. **70**, 133 (1979).
76. A. S. Gonchenko, S. V. Gonchenko, A. O. Kazakov, and A. D. Kozlov, Izv. Vyssh. Uchebn. Zaved., Prikl. Nelineinaya Din. **25** (2), 4 (2017).
77. P. V. Kuptsov, S. P. Kuznetsov, Nelineinaya Din. **2**, 307 (2006).
78. P. V. Veshchev, G. I. Guteneva, and R. S. Mukhanova, Rybn. khoz., No. 6, 45 (2010).
79. P. V. Veshchev, J. Ichthyol. **49**, 662 (2009).
80. A. I. Abakumov, L. N. Bocharov, and T. M. Reshetnyak, Vopr. Rybolov. **10**, 352 (2009).
81. I. N. Lepilina and T. I. Bulgakova, Tr. VNIRO **177**, 58 (2019).
82. A. E. Bobyrev, E. A. Kriksunov, and T. I. Kuga, J. Ichthyol. **45**, 782 (2005).
83. A. S. Maslakov, T. K. Antal, G. Yu. Riznichenko, and A. B. Rubin, Biophysics (Moscow) **61**, 387 (2016).
84. T. J. Murchie, A. J. Monteath, M. E. Mahony, et al., Nat. Commun. **12**, 7120 (2021). https://doi.org/10.1038/s41467-021-27439-6
85. V. A. Dubrovskaya, Probl. Mekh. Upr.: Nelineinye Din. Sist. **49**, 8 (2017).
86. J. M. Murray, G. R. Kaufmann, and P. D. Hodgkin, Immunol. Cell Biol. **81**, 487 (2003). https://doi.org/10.1046/j.1440-1711.2003.01191.x
87. F. Schmidt, Y. Weisblum, M. Rutkowska, et al., Nature **600**, 512 (2021). https://doi.org/10.1038/s41586-021-04005-0

Translated by E. Puchkov